Whole genome bisulfite sequencing of sperm reveals differentially methylated regions in male partners of idiopathic recurrent pregnancy loss cases

Delna Irani, M.Sc.,[a] Nafisa Balasinor, Ph.D.,[a] Vandana Bansal, M.D.,[b] Deepti Tandon, M.D.,[c] Anushree Patil, M.D.,[c] and Dipty Singh, Ph.D.[a]

[a] Department of Neuroendocrinology, ICMR - National Institute for Research in Reproductive and Child Health, Mumbai, India; [b] Department of Obstetrics and Gynaecology, Nowrosjee Wadia Maternity Hospital, Mumbai, India; and [c] Department of Clinical Research, ICMR - National Institute for Research in Reproductive and Child Health, Mumbai, India

Objective: To study the genome wide alterations in sperm DNA methylation in male partners of idiopathic recurrent pregnancy loss (iRPL) cases and note regions as potential diagnostic markers.
Design: Case-control study and methylome analysis of human sperm.
Setting: Obstetrics and Gynaecology clinics.
Patient(s): Control group consists of apparently healthy fertile men having fathered a child within the last 2 years (n = 39); and case group consists of male partners of iRPL cases having ≥2 consecutive 1st trimester pregnancy losses (n = 47).
Intervention(s): None.
Main Outcome measure(s): Sperm DNA samples of controls and cases were selected for whole genome bisulfite sequencing analysis based on the previously set thresholds of global methylation levels and methylation levels of imprinted genes (*KvDMR* and *ZAC*). Whole genome bisulfite sequencing of selected sperm genomic DNA was performed to identify differentially methylated CpG sites of iRPL cases compared with fertile controls. Pathway analysis of all the differentially methylated genes was done by Database for Annotation, Visualization, and Integrated Discovery annotation tool and Kyoto Encyclopedia of Genes and Genomes tool. Differentially methylated CpGs within genes relevant to embryo and placenta development were selected to further validate their methylation levels in study population by pyrosequencing.
Result(s): A total of 9497 differentially methylated CpGs with highest enrichment in intronic regions were obtained. In addition, 5352 differentially methylated regions and 2087 differentially methylated genes were noted. Signaling pathways involved in development were enriched on pathway analysis. Select CpGs within genes *PPARG*, *KCNQ1*, *SETD2*, and *MAP3K4* showed distinct hypomethylated subpopulations within iRPL study population.
Conclusion(s): Our study highlights the altered methylation landscape of iRPL sperm, and their possible implications in pathways of embryo and placental development. The CpG sites that are hypomethylated specifically in sperm of iRPL subpopulation can be further assessed as predictive biomarkers. (Fertil Steril® 2023;119:420-32. ©2022 by American Society for Reproductive Medicine.)
El resumen está disponible en Español al final del artículo.

Key Words: Idiopathic recurrent pregnancy loss, sperm DNA methylation, whole genome bisulfite sequencing, embryo development, placenta development

Loss of ≥2 consecutive pregnancies before the 20th week of gestation is termed as recurrent pregnancy loss (RPL). Globally, RPL has been observed to affect approximately 1%–2% of woman (1). However, in case of the Indian population, a higher prevalence of RPL of 7.46% has been reported (2). Known contributing factors to the condition of RPL include maternal factors such as uterine anatomical defects, hormonal imbalances, autoimmune disorders, thrombophilia, and infections (toxoplasma, cytomegalovirus), as well as genetic factors of both partners such as gamete aneuploidy and other

Received June 2, 2022; revised December 4, 2022; accepted December 7, 2022; published online December 14, 2022.
Supported by ICMR-NIRRCH intramural funding (Serial No. RA/1259/05-2022).
D.I. has nothing to disclose. N.B. has nothing to disclose. V.B. has nothing to disclose. D.T. has nothing to disclose. A.P. has nothing to disclose. D.S. has nothing to disclose.
Correspondence to: Dipty Singh, Ph.D., Room no. 22, Department of Neuroendocrinology, ICMR - National Institute for Research in Reproductive and Child Health, J.M. street, Parel, Mumbai 400012, India (E-mail: singhd@nirrch.res.in).

Fertility and Sterility® Vol. 119, No. 3, March 2023 0015-0282/$36.00

https://doi.org/10.1016/j.fertnstert.2022.12.017

structural as well as numerical chromosomal abnormalities (3, 4). Even with these etiological factors, approximately 50% RPL cases are categorized as idiopathic (iRPL) (3). Previous studies have shed some light on plausible male contributions, and their association to RPL such as paternal age and a high prevalence of sperm DNA fragmentation (5, 6).

Early nuclear transplant experiments have shown the contributions of paternal genome in embryo and placenta development and has mainly been implicated to be vital in placenta formation (7, 8). This implied a crucial function of monoallelic expression (based on genomic imprinting) and biallelic expression of genes to provide optimal levels of protein expression for the developmental process. This is achieved by epigenetic marks on both parental gamete genomes. One such epigenetic regulatory mechanism is DNA methylation (9).

DNA methylation includes addition of a methyl group to the fifth position of cytosine mainly at the CpG sites. The presence or absence of this modification renders the gene either unavailable for transcription factor binding or actively transcribed in a particular cell type, i.e., it regulates gene transcription activity (10–12). Paternal contribution to the developing offspring is by sperm, and studies reported that sperm DNA methylome is vital in transmitting epigenetic information from father to offspring. Although sperm DNA methylation marks are erased and re-established de novo during germ cell and pre-implantation development, the subsequent generation can inherit approximately 20% of the methylated DNA marks (9, 13, 14).

Paternal contributions to a pregnancy failure are rarely investigated. During embryogenesis and placentation, allele specific gene expressions are crucial for the development of healthy embryos (15). An inadequate DNA methylome would hinder this interplay of gene expression and in turn the process of development. Recent study from our lab has reported global hypomethylation and aberrant methylation on few imprint control regions in sperm genomic DNA of iRPL male partners (16) indicating plausible contributory epigenetic mechanisms to embryo loss. Although epigenetic reprogramming events occur, a faulty methylome origin may further affect the expression of early embryogenesis and placentation genes. Hence, our study focused on the overall paternal sperm methylome and its possible contributions to 1st trimester RPL using the current gold standard for the study of DNA methylation, viz., the whole genome bisulfite sequencing (WGBS). The WGBS technique provides single-nucleotide resolution of all cytosines in the genome and aids in viewing any methylation landscape differences specific to the iRPL sperm. Only recent studies have used WGBS technique to study the human sperm epigenome in normal and disorder conditions (17, 18). Hence, by the use of WGBS technique, this study further aimed to get focused insights on the sperm methylation status of developmental genes which could possibly affect their embryonic and placental expression during 1st trimester pregnancy and be implicated in early embryo loss.

MATERIALS AND METHODS

Ethics Declaration

This was a multicentric study for which ethical approvals were obtained from the respective institutions: the *ICMR-National Institute for Research in Reproductive and Child Health (ICMR-NIRRCH), Parel, Mumbai* (Ref: D/ICEC/Sci-60/64/2018) and *Nowrosjee Wadia Maternity Hospital, Parel, Mumbai* (Ref: IEC/NWMH/01/2019). The signed informed consents were obtained from all the study participants.

Study Cohorts and Participant Recruitment

The study cohorts included: a control group consisting of apparently healthy fertile couples and a case group consisting of couples with iRPL having ≥ 2 1st trimester pregnancy losses. Control group participants were recruited from Family Welfare Clinic, ICMR-NIRRCH and Gynaecology and Obstetrics Department, Wadia Hospital. Case group participants were recruited from Infertility clinic, ICMR-NIRRCH and Gynaecology and Obstetrics Department, Wadia Hospital. Initially, 47 control group and 58 iRPL group couples were screened for enrolment from September 2018 to December 2021. Based on the set inclusion and exclusion criteria (Table 1), a total of 39 control and 47 case couples were then enrolled in the study.

Semen collection, analysis, and processing

Semen samples were collected from male partners after 3 to 5 days of sexual abstinence. After liquefaction at 37 °C for 30 minutes, basic semen parameters (sperm concentration, motility, and morphology) were analyzed as per the World Health Organization (WHO) criteria, (2010). Sperm concentration and motility were analyzed using Neubauer hemocytometer and computer-assisted semen analysis (Hamilton Thorne Biosciences, USA), respectively. Sperm morphology was assessed as per the WHO (2010) recommended method using Papanicolaou staining.

The somatic cells were removed from semen samples by somatic cell lysis buffer (0.1% sodium dodecyl sulfate, 0.5% Triton X-100 in diethyl pyrocarbonate water) treatment for 6 hours at room temperature on a shaker. Further, the treated samples were centrifuged and given a final wash with phosphate buffer saline (PBS) (19). The sperm pellets were then subjected to subsequent PBS washes. Sperm pellets were stored at −80 °C for further use.

Sperm genomic DNA extraction

Genomic DNA was extracted from 5 million sperm using the HiPurA Sperm Genomic DNA Purification Kit (HiMedia, India) as per manufacturer's manual (16). DNA was eluted in nuclease free water and its concentration and purity (260nm/280nm = approximately, 1.7–1.8) were estimated

TABLE 1

Inclusion and exclusion criteria for participant enrolment

	Inclusion criteria	Exclusion criteria
Control: Apparently healthy fertile couples	Couples who have a child within 2 y before enrolment Males of age 21–45 y and Females of age18–35 y	Couples who have a history of infertility and miscarriage History of male infertility or RPL or abnormal semen parameters as per the *World Health Organization* 2010 standards Male partners having clinicals varicocele, occupational exposure of chemical and radiation
Case: couples with idiopathic RPL	Couples who experienced loss of ≥2 consecutive pregnancies on/before first trimester of gestation in female partners Males of age 21–45 y and Females of age18–35 y	Known contributory female factors of RPL: Anatomic defects of the uterus; Abnormal hormone levels (e.g., thyroid stimulating hormone, luteinizing hormone, follicle-stimulating hormone); Autoimmune disorders (e.g., Lupus, anticardiolupin antibodies); thrombophilia; infections (e.g. PID, HIV, CMV) Genetic factors in both partners Male partners having clinical varicocele, occupational exposure of chemicals and radiation Secondary infertility (having prior live child)

CMV = cytomegalovirus; HIV = human immunodeficiency virus; PID = pelvic inflammatory disease; RPL = recurrent pregnancy loss.

Irani. Sperm methylome in recurrent pregnancy loss. Fertil Steril 2023.

using microplate reader (Agilent BioTek, USA). The DNA samples were stored at −20 °C until further use.

Global 5mC Estimation and Bisulfite Pyrosequencing

The global 5mC content of sperm DNA was assessed using 5mC DNA ELISA kit from Zymo Research (Irvine, CA, USA) as per manufacturer's manual. Briefly, 100 ng of sperm genomic DNA samples were mixed with coating buffer, denatured, and subjected to blocking. Anti-5mC antibody along with secondary antibody solutions were added. Horse radish peroxidase developer was then added to the wells, and the absorbance was read in a plate reader at 450 nm. Standard curve ranging from 0 to 100% 5mC content was also generated from provided DNA controls, and relative global methylation levels were calculated.

All sperm genomic DNA samples were subjected to bisulfite modification using MethylCode Bisulfite Conversion Kit (Invitrogen, USA) as per manufacturer's manual. Briefly, 800 ng of genomic DNA was subjected to the processes of denaturation, sulfonation, deamination, and desulfonation in the order which converted the unmethylated cytosines to uracil with no conversions of the methylated cytosines. Modified DNA was eluted in 14 μL nuclease free water and used for loci specific polymerase chain reaction (PCR) amplification.

Primers (Sigma Aldrich, USA) were designed using the Qiagen Pyromark assay design software. Target amplification was done using Pyromark PCR Amplification Kit (Qiagen, Hilden, Germany), and PCR products were then bound to streptavidin-coated Sepharose Beads (GE Healthcare, Uppsala, Sweden) as per manufacturer's instructions (16). Further, sequencing was performed by pyro sequencer PyroMark Q96 ID (Qiagen), and sequencing results were analyzed by Pyromark Q96 software (16).

Screening for Somatic Cell Contamination

The somatic cell contamination was further ruled out by analyzing the differentially methylated *DLK1* region. This region reported by Jenkins et al. (20) in 2018 is known to be methylated in the somatic cells and unmethylated in the sperm cells. Ten CpG sites within the region Chr14:100,726,514-100,726,609 (within the *DLK1* CpG island) were analyzed by pyrosequencing (Supplemental Table 1, available online).

Sample Selection for WGBS

We screened the methylation status of sperm DNA of both groups for appropriate sample selection for WGBS. Recently reported sperm abnormal methylome markers with set thresholds (by Receiver Operating Characteristic analysis) in iRPL conditions by Khambata et al. (16) in 2021 were considered for screening purpose. 20 control and 24 iRPL samples were screened initially. According to the 5mC levels obtained and the set thresholds with abnormal iRPL sperm levels being <0.3897 % (16), sperm genomic DNA samples for respective control and case groups were selected. Additionally, the methylation status of the imprinted regions *KvDMR* and *ZAC* were analyzed by pyrosequencing. The thresholds set for iRPL conditions for locus specific methylation levels *KvDMR* and *ZAC* were >4.833 % and >3.833 %, respectively (16) that further aided the selection of total 5 control and 5 iRPL samples for the WGBS analysis. Details and features of the selected participant samples are mentioned in Supplemental Table 2 (available online).

Library Preparation and WGBS

Based on the above-described criteria, sperm genomic DNA samples (5 samples per group) were pooled for WGBS sequencing. Library preparation was done using EZ DNA Methylation Gold Kit, Zymo Research (Irvine, CA, USA). After

TABLE 2

Participant characteristics and semen analysis of control and idiopathic recurrent pregnancy loss group (mean ± standard deviation).

Characteristics	Control group	Idiopathic recurrent pregnancy loss group	*P* value
Male partners:			
Age (y)	33.15 ± 4.97	34.15 ± 5.52	.641
Sperm concentration (millions/mL)	85.85 ± 65.6	88.33 ± 54.88	.343
Sperm motility (%)	70.39 ± 19.34	64.49 ± 16.91	.063
Sperm morphology (%)	7.33 ± 2.38	8.65 ± 2.62	.13
Smokers/Tobacco users (%)	~18	~23	
Female partners:			
Age (y)	27.72 ± 4.59	29.2 ± 4.02	.253
Smokers/Tobacco users (%)	~5	~2	

Irani. Sperm methylome in recurrent pregnancy loss. Fertil Steril 2022.

performing quality control, the WGBS library was sequenced using Illumina HiSeq 2500 (Sandor, Hyderabad, India).

Whole Genome Bisulfite Sequencing Data Procession and Analysis Pipeline

The WGBS raw reads were aligned with hg38 (*Homo sapiens*) reference genome using the alignment tool Bismark (v0.14.3). Further, methylKit v1.2.4 "R" package was used for DNA methylation analysis. All CpGs covered by at least 10 reads were used for downstream analysis, with sequencing depth of 30×. The minimum mapping quality was considered at 20.

Differentially methylated CpGs (DMCs) were identified with ≥25% methylation change with q-value ≤0.05 and were used for further analysis. Summation and annotation of the genomic coordinates was done using genomation v1.18.0 ("R" package). With identification of hyper and hypo methylated sites and regions, annotation was done using University of California Santa Cruz & Ensembl databases. Based on the location of the DMC, it was annotated to be either within promoter, intron, exon, 3' end, or intergenic regions. Promoters were demarcated as the regions 2 kb upstream and downstream of the transcription start site of the reference genome. Differentially methylated regions (DMRs) were selected as a 250 bp region harboring at least 5 CpGs with average methylation ≥25% and q-value ≤0.05.

Analysis Wizard tool of **Database for Annotation, Visualization, and Integrated Discovery** (DAVID) Bioinformatics Resources (2021 update, NIAID/NIH) was used for the analysis of enriched pathways of biological processes, cellular components, and molecular functions (https://david.ncifcrf.gov/tools.jsp). Kyoto Encyclopedia of Genes and Genomes (KEGG) pathway analysis was performed by KEGG Mapper v5.0 software (https://www.kegg.jp/kegg/mapper/color.html).

Validation of DNA Methylation Levels in Study Population by Bisulfite Pyrosequencing

As described above, sperm genomic DNA of both groups were bisulfite converted and the loci specific DMC methylation levels were assessed by pyrosequencing method. The primers (Sigma Aldrich, USA) used are mentioned in Supplemental Table 1.

Statistics

Statistical analysis of study population DMCs was done using nonparametric *t* test with Welch's correction and significance level set at $P \leq .05$ using GraphPad Prism v.8.

RESULTS

Participant Characteristics, Semen Parameters, and Sperm Sample Purity

There was no significant difference in the mean values of the age of male and female partners enrolled in this study. In addition, the percentage of smokers and tobacco users was similar in both groups (Table 2). Semen parameters of both groups were within the normal range as per the WHO (2010) reference values. No significant differences in semen volume, pH, sperm count, motility, and morphology, were observed. Efficiency of somatic lysis buffer treatment in sperm samples was checked by *DLK1* methylation analysis in comparison with blood DNA samples. The sperm DNA samples used for analysis were found to be pure (Supplemental Fig. 1, available online).

DNA Methylation Mapping by WGBS

Data by WGBS was generated from the pooled bisulfite converted sperm DNA of control and iRPL groups. After filtering raw reads, approximately 102.9 GB data was processed (Supplemental Table 3, available online). These clean reads were then mapped to the human reference genome (hg38) with a mapping efficiency of 74.9% in control and 74.2% in iRPL groups (Supplemental Table 4, available online).

The methylated cytosine of the genome can be divided into 3 types: CG, CHG, and CHH (H = A, C or T). The whole genome methylated cytosine levels in the control group were 97.29% CGs, 0.68 % CHGs, and 2.03% CHHs, whereas those in the iRPL group were 97.31% CGs, 0.68% CHGs, and 2.01% (Fig. 1A). In addition, in case of methylated CGs from total CGs was 80% in control and 80.2 % in iRPL group, methylated CHGs from total CHGs was 0.10% in both groups, and methylated CHHs from total CHHs was also found to be 0.10% in both the groups (Supplemental Table 4).

FIGURE 1

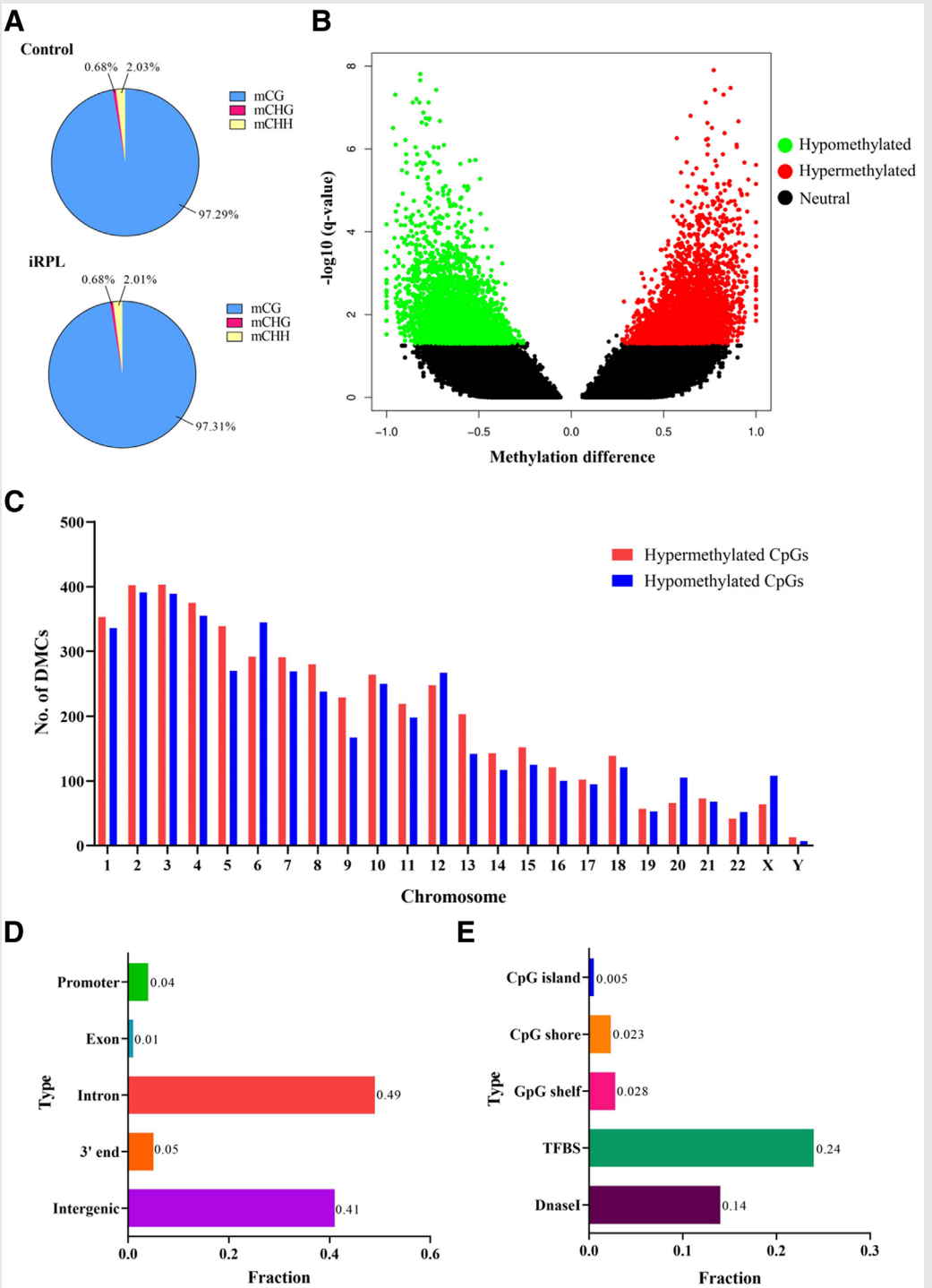

(**A**) Percentage of deoxyribonucleic acid methylation types from total methylated cytosines in the sperm whole genome in control and iRPL groups (H = A, G or T). The methylated cytosines in the CG context (mCG), methylated cytosines in the CHG context (mCHG) and methylated cytosines in the CHH context (mCHH) are denoted by blue, pink and yellow colors respectively; Differentially methylated CpGs (DMCs) analysis based on the cut-offs of ≥ 25% methylation difference and q-value ≤ 0.05: (**B**) Volcano plot representing the distribution of DMCs as hypermethylated or hypomethylated, -log10 (q-value) vs. fraction of methylation difference. (**C**) Chromosome-wise distribution of hypermethylated and hypomethylated DMCs, (**D**) Fraction of DMCs within promoter, exon, intron, 3′ end and intergenic regions and (**E**) Fraction of DMCs within CpG island, CpG shore, CpG shelf, transcription factor binding sites and DnaseI hypersensitive regions.

Irani. Sperm methylome in recurrent pregnancy loss. Fertil Steril 2023.

FIGURE 2

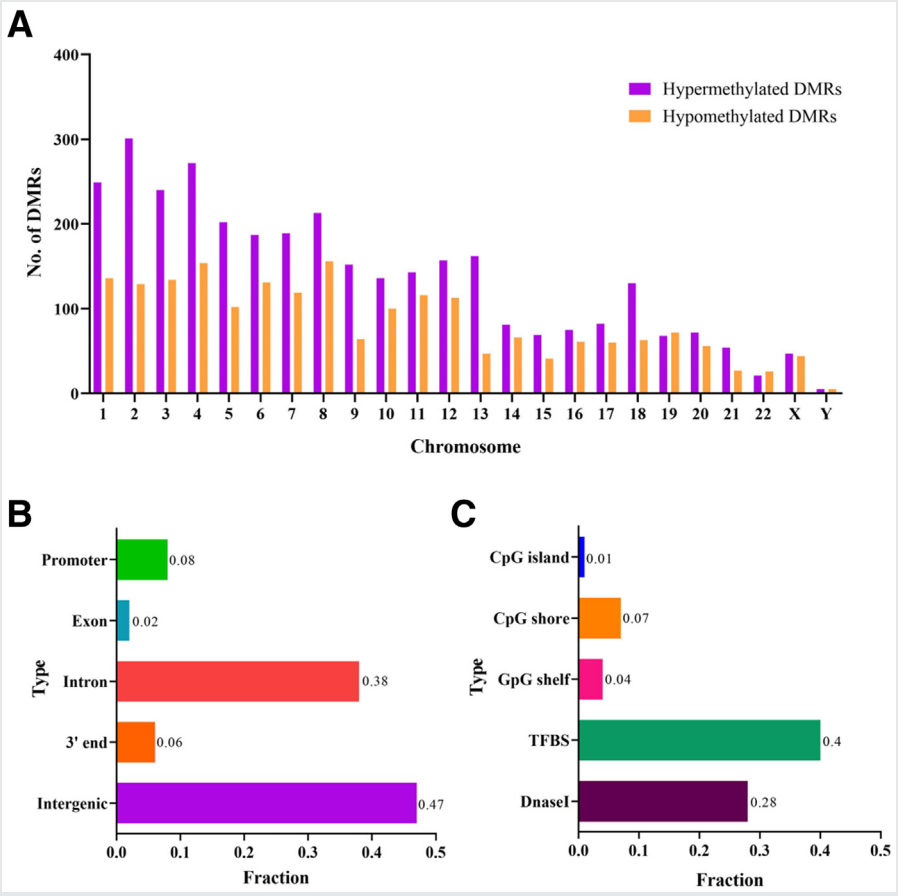

Differentially methylated regions (DMRs) analysis based on the cut-offs of ≥ 25% average methylation difference and q-value ≤ 0.05: (**A**) Chromosome-wise distribution of hypermethylated and hypomethylated DMRs, (**B**) Fraction of DMRs within promoter, exon, intron, 3′ end and intergenic regions and (**C**) Fraction of DMRs within CpG island, CpG shore, CpG shelf, transcription factor binding sites and DnaseI hypersensitive regions.

Irani. Sperm methylome in recurrent pregnancy loss. Fertil Steril 2023.

DMC Analysis

Based on the set cut-offs, a total of 9497 DMCs were obtained, from which 4609 DMCs were hypomethylated and 4888 DMCs were hypermethylated. Their distribution based on methylation difference values and q-values are represented as volcano plot (Fig. 1B). Further details of DMCs including locations, annotations, and methylation percentage are provided in Supplemental Table 5 (available online). The chromosome-wise distribution of these hypo and hypermethylated DMCs were similar on each chromosome (Fig. 1C and Supplemental Table 5). Based on alignment, DMCs were found to be enriched in promoters, exons, introns, 3' end, and intergenic regions (Fig. 1D) and in features such as CpG islands, GpG shores, CpG shelves, Transcription Factor Binding Sites (TFBS) and DnaseI hypersensitive regions (Fig. 1E) (Supplemental Table 6, available online). The fractions represent the amount of DMCs with the signature feature from the total DMCs. Highest enrichment was observed in the intronic and intergenic regions and in the TFBS regions.

DMR Analysis

A total of 5352 DMRs were obtained with 2035 DMRs hypomethylated and 3317 DMRs hypermethylated (Supplemental Table 7, available online). Here, we observed a higher number of hypermethylated DMRs than the hypomethylated DMRs. The chromosome-wise distribution also displayed high proportion of hypermethylated DMRs (Fig. 2A). On alignment, DMRs enriched in promoters, exons, introns, 3' end, and intergenic regions (Fig. 2B) and in features such as CpG islands, GpGs shores, CpG shelves, TFBS, and DnaseI hypersensitive regions (Fig. 2C) (Supplemental Table 8, available online) were observed. Highest DMRs enrichment was observed in the intergenic and intronic regions and in TFBS regions.

Differentially Methylated Genes Functional Annotations

The Differentially methylated genes (DMGs) were identified by DMCs present within intron, exon, promoter, and 3'

FIGURE 3

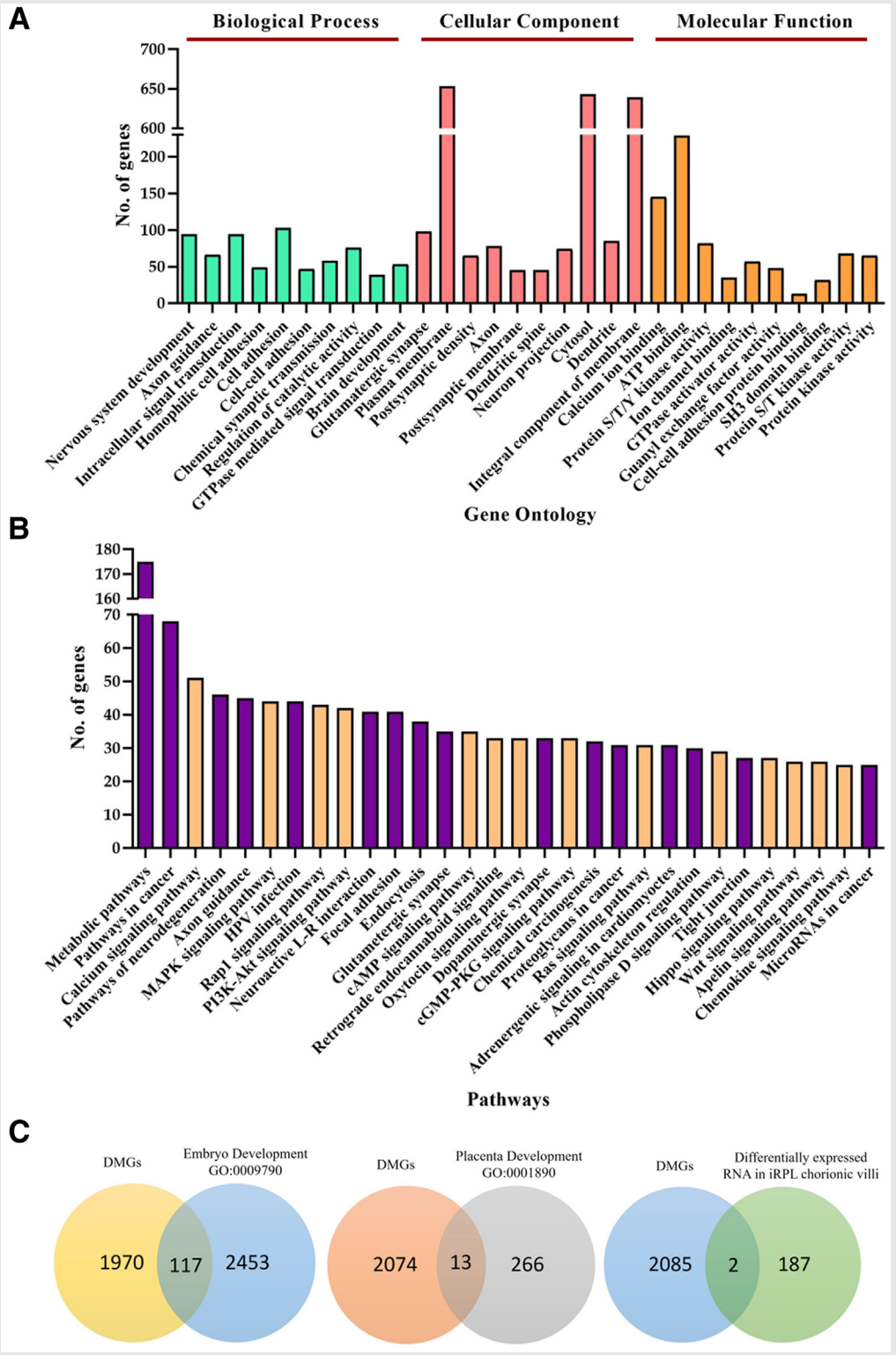

Differentially methylated genes (DMGs) annotations: (**A**) Top 10 enriched pathways of biological processes, cellular components, molecular functions on gene ontology analysis using DAVID bioinformatics tool (Bonferroni test, $P \leq .05$). (**B**) Top 30 pathways by KEGG mapper tool with signaling pathways highlighted as orange bars. (**C**) DMGs common to human embryo development (GO:0009790), placenta development (GO:0001890) and differentially expressed RNA in iRPL 1st trimester chorionic villi.

Irani. Sperm methylome in recurrent pregnancy loss. Fertil Steril 2023.

UTR features. A total of 2087 DMGs were identified with gene list provided (Supplemental Table 9, available online). To get insights on the functions of these genes, gene ontology (GO) was obtained using DAVID bioinformatics tools and pathway analysis was done using KEGG mapper. In case of GO analysis, "Direct" pathways were selected. Using Bonferroni test and $P \leq .05$, top 10 pathways of biological processes, cellular components, and molecular functions are represented (Fig. 3A). Nervous system development (94 DMGs), axon guidance (66 DMGs), and intracellular signal transduction (94 DMGs) were the most enriched pathways under biologic processes; the most enriched cellular components were glutamatergic synapse (98 DMGs), plasma membrane (653 DMGs), and postsynaptic density (65 DMGs); and the top enriched molecular functions were calcium ion binding (145 DMGs), ATP binding (229 DMGs), and protein serine/threonine/tyrosine kinase activity (82 DMGs). On KEGG pathway analysis, the top pathways included many developmental signaling pathways such as calcium, MAPK, Rap1, Ras, Wnt, and Hippo signaling pathways. These pathways have been highlighted among the top 30 pathways on KEGG analysis (Fig. 3B).

Furthermore, RPL is attributed to abnormalities in embryo and/or placenta development. To select genes for validation among the study population, we obtained DMGs involved in the pathways of *embryo development* (GO:0009790) and *placenta development* (GO:0001890) using the website *Gene List Venn Diagram* (http://genevenn.sourceforge.net/). A total of 117 DMGs involved in embryo development and 13 DMGs involved in placenta development were obtained (Fig. 3C). Gene lists of these DMGs is provided in Supplemental Table 10 (available online). In addition, we screened DMGs common to differentially expressed genes in chorionic villi of iRPL 1st trimester placenta (21). However, we obtained only 2 DMGs; namely *PRELI domain containing 1* (*PRELID1*) and *phosphatidylinositol glycan anchor biosynthesis class T* (*PIGT*) common to the RNA-sequencing data (Fig. 4C and Supplemental Table 10). Based on a previous study which enlisted human trophoblast subtype specific gene expression (markers, hormone genes, and transcription factors) by single-cell RNA-sequencing method (22), we also obtained DMGs common to them. A total of 35 trophoblast markers, 14 transcription factors, and 4 hormone genes were obtained (Supplemental Table 11, available online).

Methylation Status of Selected DMGs in Study Population

The DMGs common to the pathways of *embryo development* (GO:0009790) and *placenta development* (GO:0001890) were further screened individually using University of California Santa Cruz browser. The DMCs having any regulatory features such as promoters, proximal, and distal enhancers were mainly selected for validation within the population. Out of these, 10 DMCs were selected which were located within the genes *peroxisome proliferator activated receptor gamma* (*PPARG*), *potassium voltage-gated channel subfamily Q member 1* (*KCNQ1*), *homeobox C4* (*HOXC4*), *mitogen-activated protein kinase 14* (*MAPK14*), *mitogen-activated protein kinase kinase kinase 4* (*MAP3K4*), *DNA methyltransferase 1* (*DNMT1*), *SET domain containing 2, histone lysine methyltransferase* (*SETD2*), *insulin like growth factor 2 receptor*

FIGURE 4

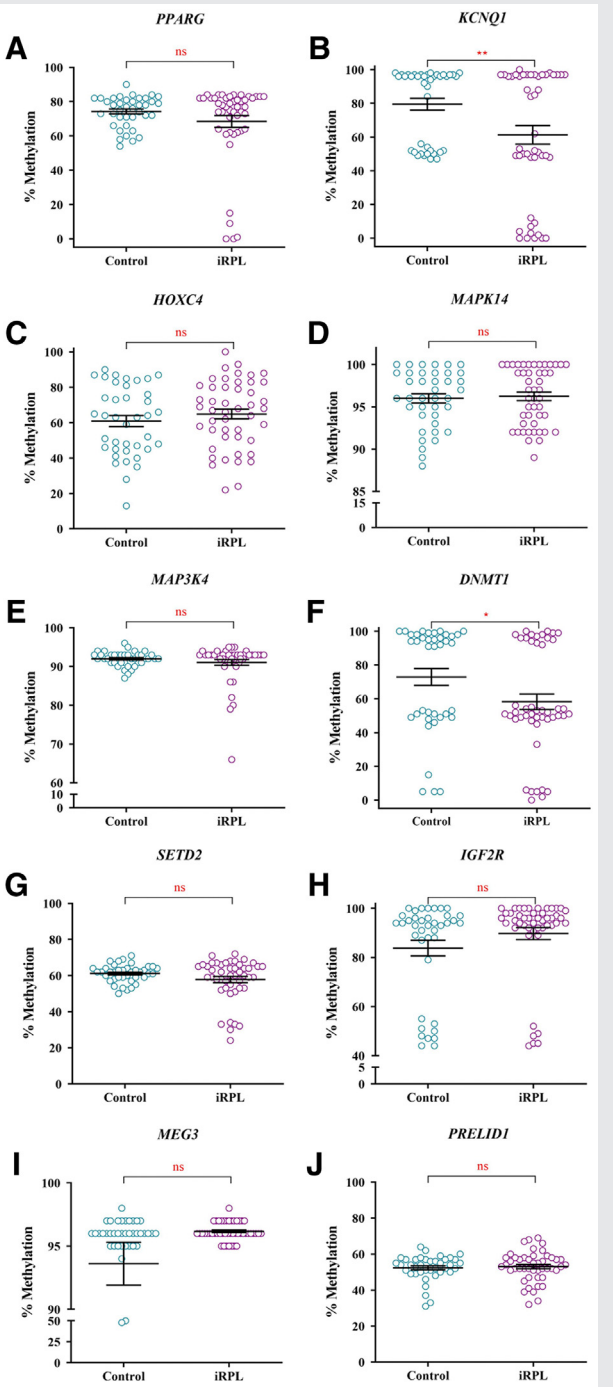

Population-wide methylation status of selected DMCs within genes (**A**) *PPARG*, (**B**) *KCNQ1*, (**C**) *HOXC4*, (**D**) *MAPK14*, (**E**) *MAP3K4*, (**F**) *DNMT1*, (**G**) *SETD2*, (**H**) *IGF2R*, (**I**) *MEG3* and (**J**) *PRELID1*. Mean ± SE. Control (n = 39) vs. iRPL (n = 47) (*$P \leq .05$, **$P \leq .01$, ns – not significant).

Irani. Sperm methylome in recurrent pregnancy loss. Fertil Steril 2023.

(*IGF2R*), and *maternally expressed 3* (*MEG3*). In addition, *PRELID1* was selected among the common DMGs with RNA-sequencing data of 1st trimester iRPL chorionic villi (21). Features of each DMC are mentioned in Supplemental Table 12 (available online). Validation of the pooled sample was done, and the methylation difference (hypo or hyper) of selected DMCs obtained by WGBS were reflected in the same pooled samples by pyrosequencing despite these 2 techniques having different sensitivity (Supplemental Fig. 2, available online).

A total of 39 control and 47 iRPL sperm bisulfite converted DNA samples were subjected to pyrosequencing for the above mentioned DMCs. A subpopulation of approximately 10.63% of the total iRPL population showed hypomethylation of the *PPARG* DMC in the range of 0 to 15%. However, no significant hypomethylation ($P=.123$) was observed in the total iRPL population compared with the control group (Fig. 4A). In case of *KCNQ1* DMC, a subpopulation of 23.4% of the total iRPL population exhibited hypomethylation in the range of 0 to 12%. Overall, there was significant difference ($P=.006$) in the methylation status of the *KCNQ1* DMC compared with control (Fig. 4B). As for *HOXC4* and *MAPK14* DMCs, methylation levels of both populations were comparable to each other with no significant differences ($P=.343$, $P=.751$) (Fig. 4C and 4D). A subpopulation of 8.51% of the total iRPL population exhibited slight hypomethylation of the *MAP3K4* DMC in the range of 66%–82% with no significant difference ($P=.248$) in the overall iRPL group compared with control (Fig. 4E). Significant hypomethylation ($P=.031$) was observed in the *DNMT1* DMC in the overall iRPL population (Fig. 4F). *SETD2* DMC methylation analysis noted a subpopulation of 12.76% of the total iRPL population showing hypomethylation in the range of 24%–34%. However, no significant hypomethylation ($P=.074$) was observed in the total iRPL population compared with control (Fig. 4G). *IGF2R* DMC was a hypermethylated DMC and overall nonsignificant hypermethylation ($P=.146$) was observed in the iRPL group compared with control (Fig. 4H). *MEG3* was also a hypermethylated DMC, and all iRPL samples had high methylation levels (Fig. 4I). Overall, nonsignificant hypermethylation ($P=.139$) was observed in the iRPL population compared with control. Methylation levels of *PRELID1* DMC were similar in both groups ($P=.711$) (Fig. 4J).

DISCUSSION

Recurrent pregnancy loss is mainly attributed to inadequate development of the fetus and placenta during gestation. With the advent of the knowledge that paternal genome is crucial for placental development (7, 8), and during epigenome reprogramming of the pre-implantation embryo, upto 20% DNA methylation marks are retained on the paternal alleles (9, 13, 14); it raises the question whether paternal epigenome could truly be one of the reasons for faulty placentation and embryogenesis leading to early embryo loss. In addition, DNA methylation has been usually associated with transcriptional silencing; however, the effect of methylation on binding affinity for most transcription factors (TFs) is still quite elusive (23). Interestingly, a recent study has elucidated on the increased or decreased binding affinity of different human TFs to methylated regions based on their locations in the binding site (24). Hence, differential methylation of the sperm genome could be crucial in expression of genes in the primary stages of embryo and placenta development.

A previous study from our lab reported significant global DNA hypomethylation, hypomethylation of paternally imprinted DMRs *IGF2-H19 DMR* and *IG-DMR*, and hypermethylation of maternally imprinted DMRs *MEST*, *ZAC*, *KvDMR*, *PEG10*, and *PEG3* in spermatozoa of iRPL male partners (16). This study gave insights on the plausible aberrant methylation of known imprint control regions affecting the process of embryo and placenta development. Furthermore, to obtain the genome wide methylation status of CpG sites of the iRPL sperm genome with methylation difference with that of healthy fertile sperm genomes, WGBS was performed. It was essential to carry out the initial screening by 5mC analysis (global hypomethylation in iRPL) and methylation analysis of the maternally imprinted regions of *KvDMR* and *ZAC* (hypermethylated in iRPL) based on previously set methylation thresholds (16), as it is likely that only a fraction of the iRPL cases would have paternal epigenetic contributions. It is expected, as we also cannot account for possible unknown female factors responsible for RPL. However, the limitation of selecting only 5 samples from iRPL group could be that we might have missed out other probable novel DMCs of wider iRPL population.

On WGBS analysis, highest DMC enrichment was noted in the TFBS and intronic regions of the iRPL genome. Recent studies have predicted the regulatory role of introns in certain gene expressions and have proposed that enhancer sequences are present in them which allow TF binding (25, 26). Interestingly, the overlap of DMCs within TFBS and intronic DMCs was the highest compared with intergenic, 3'end, and promoter DMCs. Some of the 250bp DMRs were observed to be adjacent to each other which would form large DMRs. The obtained DMRs were also highly enriched within intronic regions and TFBS. In retrospect, investigating these DMCs and DMRs within these highly enriched regions in the sperm iRPL population would be intriguing.

To get insights on which expression pathways during first trimester pregnancy could possibly be affected in iRPL because of paternal epigenome, we chose the DMGs as input. Gene ontology using the DAVID functional annotation tool was performed, and a list of enriched biological processes, cell components, and molecular functions were obtained. Similar pathways were noted on KEGG analysis. In addition, the major developmental signaling pathways of MAPK, Rap1, PI3K-Akt, cAMP, Ras, Hippo, and Wnt were among the top 30 pathways by KEGG analysis. Besides fetal development, the cell signaling pathways MAPK, PI3K-Akt, Wnt, and cAMP are found to be involved during invasion and syncytialization of the trophoblast cells which is an essential process in the implantation of embryo and placenta development (27). PI3K-Akt signaling pathway is involved in the trophoblast decidua invasion, especially during early pregnancy (28). Similarly, Ras signaling pathway regulates the phosphorylation and destabilization of proapoptotic proteins responsible for

trophoblast stem cell survival (29). Placental cell fusion is regulated by the other 2 signaling pathways, Rap1 and cAMP (30, 31). These analyses have highlighted the involvement of DMGs specific to early iRPL involved in pathways important for in utero development.

To narrow down the DMGs specific to our condition, we further filtered DMGs common to the human embryo and placenta development processes. Among these, we preferred selecting the DMGs having DMCs within the regulatory regions such as enhancer or promoter feature and TFBS for validation in the pooled samples as well as the entire study population. Among the 10 selected DMCs, few showed either a subpopulation or overall significant methylation difference. Moreover, PPARγ expression is mainly observed in early trophoblast cells of placenta and modulates the differentiation of the trophoblast cells (22, 32). The trophoblast invasion is negatively correlated to PPARγ stimulation (33). In case of RPL, significantly higher expression of PPARγ was identified in the extravillous trophoblast of 1st trimester placental villi (34). Now, we have reported one *PPARG* intronic DMC which shows low to no methylation in a subpopulation specific to the iRPL group. In addition, it was within a TFBS and suggests a possible regulatory role in PPARγ expression during placental development. Its hypomethylated status in iRPL could be the reason to its higher expression in spontaneous abortion villi reported in the previous study.

Another DMC showing a significant distinct subpopulation in the iRPL group was within the *KCNQ1* gene. The major imprint control region of *KvDMR* within intron 10 of *KCNQ1* gene controls the expression of 6 maternally expressed genes of which some are involved in placental growth and development, and the paternally expressed lncRNA transcript *KCNQ1 opposite strand/antisense transcript 1* (*KCNQ1OT1*) (35). *KCNQ1OT1*, during fetal development, silences the expression of the other genes of *KvDMR* cluster (36). Hypomethylation of the *KvDMR* region in iRPL sperm has been previously reported (16). However, our DMC was within intron 11 of *KCNQ1* and upstream to *KCNQ1OT1*. This DMC lies within the enhancer sequence for *KCNQ1OT1* gene and has TFBS for multiple TFs. This DMC showed the largest hypomethylated subpopulation and seems to be a promising paternal factor predictive biomarker for RPL.

Regarding the DMCs of epigenetic regulator genes *SETD2* and *DNMT1*, we noted methylation differences in the iRPL group compared with controls. The predominant histone methyltransferase in mammals SETD2 has been reported to regulate coronary vascular and blood vessel development in embryonic mouse hearts and its loss led to fetal lethality (37). Importantly, SETD2 has been reported to regulate the maternal epigenome, genomic imprinting, and embryonic development (38). The *SETD2* DMC we obtained had an enhancer signature and with a distinct hypomethylated iRPL subpopulation, there is a possibility of its implication in aberrant SETD2 expression in utero of iRPL cases. Moreover, DNMT1 is crucial for the maintenance of methyl marks in actively dividing cells of the placenta and fetus (39). However, *DNMT1* DMC did not show a distinct hypomethylated iRPL population from that of control, rendering not much implication of this DMC specific to iRPL.

We also evaluated hypermethylated imprinted gene DMCs of *IGF2R* and *MEG3* (40), and noted an overall hypermethylation in the study population. During the first trimester, IGF2 bound IGF2R stimulates extravillous trophoblast cells for migration (41), and *MEG3* lncRNA inactivation in embryonic villi has been implicated in iRPL (42). However, we could report no aberrant methylation of these CpGs in sperm specific to the iRPL population.

HOXC4 is part of the group of homeobox genes implicated in the morphogenesis of embryos (43). The *HOXC4* DMC was also a part of the *HOXC6* gene. However, no iRPL specific sperm methylation patterns were observed for this DMC. The DMCs for the MAPK pathway genes *MAPK14* and *MAP3K4* were also selected for study population analysis. MAPK14 is attributed to be essential for trophoblast stem cell differentiation, and increased MAPK14 expression in placental villi has been reported in recurrent miscarriage (44, 45). However, we could not report any iRPL specific aberrant sperm methylation for the *MAPK14* DMC. Loss of MAP3K4 results in trophoblast defects leading to hyper invasion, defective decidualization, fetal growth restriction, and implantation defects along with other embryonic defects (46, 47). In addition, MAP3K4 regulates histone H2B Acetylation and in turn maintains epithelial state in trophoblast stem cells (48). Our study reports iRPL subpopulation of hypomethylated *MAP3K4* DMC. This DMC also has a distal enhancer signature and could be a key regulatory region for *MAP3K4* expression. *PRELID1* was found to be under expressed during the 1st trimester iRPL chorionic villi (21) as well as was hypomethylated in sperm DNA according to the WGBS analysis. However, no significant methylation difference was observed to implicate its paternal contribution in iRPL.

Overall, this study notes DNA methylome alterations in the iRPL sperm with 4 promising regions as diagnostic markers.

CONCLUSION

This study highlights the differentially methylated landscape of iRPL sperm genome compared with the fertile group. The differentially methylated genes also aided in recognizing the developmental pathways that were affected, possibly contributing to RPL pathology. Among the varied differentially methylated genes, we were able to identify some that could be taken up further for validation in a large population and assessed for potential diagnostic markers in the sperm of iRPL male partners. In addition, this study strengthens the understanding of involvement of the paternal epigenome in maintenance of pregnancy and fetal growth and development.

Acknowledgments: The authors are grateful to all the study participants for their consent and cooperation. The authors thank Niti Singh (B.Tech.) for her invaluable aid in WGBS analysis. We also gratefully thank Deepshikha Arya (M.Sc.), Sunita Kharat (B.A.), Sharmila Kamat (M.S.W.), Suryakant Mandavkar (B.Sc., D.M.L.T.), Tejashree Sontakke (M.S.W.), Shobha Sonawane (M.Sc., D.M.L.T), Reshma Goankar (M.Sc., D.M.L.T), Swati Jadhav (B.Sc., D.M.L.T), and Deepak Shelar (S.S.C.) for their assistance in participant recruitment.

The authors thank Sharvari Deshpande (Ph.D.) and Kushaan Khambata (Ph.D.) for their valuable inputs in planning of experiments. Delna Irani thanks Lady Tata Memorial Trust for her research fellowship.

REFERENCES

1. Bender Atik R, Christiansen OB, Elson J, Kolte AM, Lewis S, Middeldorp S, et al. ESHRE guideline: recurrent pregnancy loss. Hum Reprod Open 2018; 2018:1–12.
2. Patki A, Chauhan N. An epidemiology study to determine the prevalence and risk factors associated with recurrent spontaneous miscarriage in india. J Obstet Gynaecol India 2016;66:310–5.
3. Ford HB, Schust DJ. Recurrent pregnancy loss: etiology, diagnosis, and therapy. Rev Obstet Gynecol 2009;2:76–83.
4. Ibrahim Y, Johnstone E. The male contribution to recurrent pregnancy loss. Transl Androl Urol 2018;7(Suppl 3):S317–27.
5. Slama R, Bouyer J, Windham G, Fenster L, Werwatz A, Swan SH. Influence of paternal age on the risk of spontaneous abortion. Am J Epidemiol 2005;161: 816–23.
6. Kazerooni T, Asadi N, Jadid L, Kazerooni M, Ghanadi A, Ghaffarpasand F, et al. Evaluation of sperm's chromatin quality with acridine orange test, chromomycin A3 and aniline blue staining in couples with unexplained recurrent abortion. J Assist Reprod Genet 2009;26:591–6.
7. McGrath J, Solter D. Completion of mouse embryogenesis requires both the maternal and paternal genomes. Cell 1984;37:179–83.
8. Surani MAH, Barton SC, Norris ML. Experimental reconstruction of mouse eggs and embryos: an analysis of mammalian development. Biol Reprod 1987;36:1–16.
9. Heard E, Martienssen RA. Transgenerational epigenetic inheritance: myths and mechanisms. Cell 2014;157:95–109.
10. Borgel J, Guibert S, Li Y, Chiba H, Schübeler D, Sasaki H, et al. Targets and dynamics of promoter DNA methylation during early mouse development. Nat Genet 2010;42:1093–100.
11. Bartke T, Vermeulen M, Xhemalce B, Robson SC, Mann M, Kouzarides T. Nucleosome-interacting proteins regulated by DNA and histone methylation. Cell 2010;143:470–84.
12. Guibert S, Weber M. Functions of DNA methylation and hydroxymethylation in mammalian development. Curr Top Dev Biol 2013;104:47–83.
13. Wang L, Zhang J, Duan J, Gao X, Zhu W, Lu X, et al. Programming and inheritance of parental DNA methylomes in mammals. Cell 2014;157:979–91.
14. van Dongen J, Nivard MG, Willemsen G, Hottenga JJ, Helmer Q, Dolan CV, et al. Genetic and environmental influences interact with age and sex in shaping the human methylome. Nat Commun 2016;7:11115.
15. Plasschaert RN, Bartolomei MS. Genomic imprinting in development, growth, behavior and stem cells. Development 2014;141:1805–13.
16. Khambata K, Raut S, Deshpande S, Mohan S, Sonawane S, Gaonkar R, et al. DNA methylation defects in spermatozoa of male partners from couples experiencing recurrent pregnancy loss. Hum Reprod 2021;36:48–60.
17. Chen X, Lin Q, Wen J, Lin W, Liang J, Huang H, et al. Whole genome bisulfite sequencing of human spermatozoa reveals differentially methylated patterns from type 2 diabetic patients. J Diabetes Investig 2020;11:856–64.
18. Leitão E, Di Persio S, Laurentino S, Wöste M, Dugas M, Kliesch S, et al. The sperm epigenome does not display recurrent epimutations in patients with severely impaired spermatogenesis. Clin Epigenet 2020;12:1–15.
19. Goodrich R, Johnson G, Krawetz SA. The preparation of human spermatozoal RNA for clinical analysis. Arch Androl 2007;53:161–7.
20. Jenkins TG, Liu L, Aston KI, Carrell DT. Pre-screening method for somatic cell contamination in human sperm epigenetic studies. Syst Biol Reprod Med 2018;64:146–55.
21. Sõber S, Rull K, Reiman M, Ilisson P, Mattila P, Laan M. RNA sequencing of chorionic villi from recurrent pregnancy loss patients reveals impaired function of basic nuclear and cellular machinery. Sci Rep 2016;6:38439.
22. Liu Y, Fan X, Wang R, Lu X, Dang YL, Wang H, et al. Single-cell RNA-seq reveals the diversity of trophoblast subtypes and patterns of differentiation in the human placenta. Cell Res 2018;28:819–32.
23. Keshet I, Yisraeli J, Cedar H. Effect of regional DNA methylation on gene expression. Proc Natl Acad Sci U S A 1985;82:2560–4.
24. Yin Y, Morgunova E, Jolma A, Kaasinen E, Sahu B, Das PK, et al. Impact of cytosine methylation on DNA binding specificities of human transcription factors. HHS Public Access 2021;356:1–36.
25. Gallegos JE, Rose AB. Intron DNA sequences can be more important than the proximal promoter in determining the site of transcript initiation. Plant Cell 2017;29:843–53.
26. Blattler A, Yao L, Witt H, Guo Y, Nicolet CM, Berman BP, et al. Global loss of DNA methylation uncovers intronic enhancers in genes showing expression changes. Genome Biol 2014;15:469.
27. Kumar Gupta SK, Malhotra SS, Malik A, Verma S, Chaudhary P, Marg AA. Cell signaling pathways involved during invasion and syncytialization of trophoblast cells. Am J Reprod Immunol 2016;75:361–71.
28. Zhang X, Fu LJ, Liu XQ, Hu ZY, Jiang Y, Gao RF, et al. Nm23 regulates decidualization through the PI3K-Akt-mTOR signaling pathways in mice and humans. Hum Reprod 2016;31:2339–51.
29. Yang W, Klaman LD, Chen B, Araki T, Harada H, Thomas SM, et al. An Shp2/SFK/Ras/Erk signaling pathway controls trophoblast stem cell survival. Dev Cell 2006;10:317–27.
30. Chang CW, Cheong ML, Chang GD, Tsai MS, Chen H. Involvement of Epac1/Rap1/CaMKI/HDAC5 signaling cascade in the regulation of placental cell fusion. Mol Hum Reprod 2013;19:745–55.
31. Gerbaud P, Taskén K, Pidoux G. Spatiotemporal regulation of cAMP signaling controls the human trophoblast fusion. Front Pharmacol 2015;6:202.
32. Schaiff WT, Carlson MG, Smith SD, Levy R, Nelson DM, Sadovsky Y. Peroxisome proliferator-activated receptor-modulates differentiation of human trophoblast in a ligand-specific manner. J Clin Endocrinol Metab 2000;85: 3874–81.
33. Fournier T, Handschuh K, Tsatsaris V, Evain-Brion D. Involvement of PPARγ in human trophoblast invasion. Placenta 2007;28(Suppl A):76–81.
34. Toth B, Bastug M, Mylonas I, Scholz C, Makovitzky J, Kunze S, et al. Peroxisome proliferator-activated receptor-gamma in normal human pregnancy and miscarriage. Acta Histochem 2009;111:372–8.
35. Beatty L, Weksberg R, Sadowski PD. Detailed analysis of the methylation patterns of the KvDMR1 imprinting control region of human chromosome 11. Genomics 2006;87:46–56.
36. Du M, Beatty LG, Zhou W, Lew J, Schoenherr C, Weksberg R, et al. Insulator and silencer sequences in the imprinted region of human chromosome 11p15.5. Hum Mol Genet 2003;12:1927–39.
37. Chen F, Chen J, Wang H, Tang H, Huang L, Wang S, et al. Histone lysine methyltransferase setd2 regulates coronary vascular development in embryonic mouse hearts. Front. Cell Dev Biol 2021;9:651655.
38. Xu Q, Xiang Y, Wang Q, Wang L, Brind'Amour J, Bogutz AB, et al. SETD2 regulates the maternal epigenome, genomic imprinting and embryonic development. Nat Genet 2019;51:844–56.
39. Koukoura O, Sifakis S, Spandidos DA. DNA methylation in the human placenta and fetal growth (review). Mol Med Rep 2012;5:883–9.
40. Moore GE, Ishida M, Demetriou C, Al-Olabi L, Leon LJ, Thomas AC, et al. The role and interaction of imprinted genes in human fetal growth. Philos Trans R Soc B Biol Sci 2015;370:20140074.
41. McKinnon T, Chakraborty C, Gleeson LM, Chidiac P, Lala PK. Stimulation of human extravillous trophoblast migration by IGF-II is mediated by IGF type 2 receptor involving inhibitory G protein(s) and phosphorylation of MAPK. J Clin Endocrinol Metab 2001;86:3665–74.
42. Zhang J, Liu X, Gao Y. The long noncoding RNA MEG3 regulates Ras-MAPK pathway through RASA1 in trophoblast and is associated with unexplained recurrent spontaneous abortion. Mol Med 2021;27:70.
43. Pitera JE, Smith V, Thorogood P, Milla PJ. Coordinated expression of 3′ Hox genes during murine embryonal gut development: an enteric Hox code. Gastroenterology 1999;117:1339–51.
44. Winger QA, Guttormsen J, Gavin H, Bhushan F. Heat shock protein 1 and the mitogen-activated protein kinase 14 pathway are important for mouse trophoblast stem cell differentiation 1. Biol Reprod 2007;76:884–91.
45. Pan HT, Ding HG, Fang M, Yu B, Cheng Y, Tan YJ, et al. Proteomics and bioinformatics analysis of altered protein expression in the placental villous tissue from early recurrent miscarriage patients. Placenta 2018;61:1–10.

46. Abell AN, Granger DA, Johnson NL, Vincent-Jordan N, Dibble CF, Johnson GL. Trophoblast stem cell maintenance by fibroblast growth factor 4 requires MEKK4 activation of jun n-terminal kinase. Mol Cell Biol 2009;29: 2748–61.
47. Abell AN, Rivera-Perez JA, Cuevas BD, Uhlik MT, Sather S, Johnson NL, et al. Ablation of MEKK4 kinase activity causes neurulation and skeletal patterning defects in the mouse embryo. Mol Cell Biol 2005;25: 8948–59.
48. Abell AN, Jordan NV, Huang W, Prat A, Midland AA, Johnson NL, et al. MAP3K4/CBP-regulated H2B acetylation controls epithelial-mesenchymal transition in trophoblast stem cells. Cell Stem Cell 2011;8:525–37.

La secuenciación del genoma completo del esperma por bisulfito revela regiones metiladas en parejas masculinas de casos de pérdida idiopática.

Objetivo: Estudiar las alteraciones a nivel del genoma en la metilación del ADN espermático en parejas masculinas de casos de pérdida idiopática recurrente del embarazo (iRPL) y señalar regiones como posibles marcadores diagnósticos.

Diseño: Estudio de caso control y análisis del metiloma del esperma humano.

Lugar: Clínica de obstetricia y ginecología.

Paciente(s): El grupo control está formado por hombres fértiles aparentemente sanos que han tenido un hijo en los últimos 2 años (n= 39) y el grupo de casos está formado por parejas masculinas de casos de iRPL que han tenido $\geq$ 2 pérdidas de embarazo consecutivas en el primer trimestre (n= 47).

Intervención(es): Ninguna.

Principal(es) medida(s) de resultado(s): Se seleccionaron muestras de ADN espermático de controles y casos para el análisis de secuenciación de bisulfito de genoma completo basándose en los umbrales previamente establecidos de niveles de metilación global y niveles de metilación de genes improntados (KvDMR y ZAC). Se realizó la secuenciación de bisulfito del genoma completo del ADN genómico de espermatozoides seleccionados para identificar los sitios CpG diferencialmente metiladas de los casos de iRPL en comparación con los controles fértiles. El análisis de rutas de todos los genes diferencialmente metilados se realizó mediante la herramienta de anotación "*Database for Annotation, Visualization"*, and "*Integrated Discovery"* y la herramienta "*Kyoto Encyclopedia of Genes and Genomes"*. Las CpGs diferencialmente metiladas dentro de los genes relevantes para el desarrollo del embrión y la placenta fueron seleccionadas para validar sus niveles de metilación en la población de estudio mediante pirosecuenciación.

Resultado(s): Se obtuvo un total de 9497 CpGs diferencialmente metiladas con mayor enriquecimiento en regiones intrónicas. Además, se observaron 5352 regiones diferencialmente metiladas y 2087 genes diferencialmente metilados. Las vías de señalización implicadas en el desarrollo fueron enriquecidas en el análisis de rutas. CpGs seleccionadas dentro de los genes *PPARG, KCNQ1, SETD2* y *MAP3K4* mostraron distintas subpoblaciones hipometiladas dentro de la población de estudio iRPL.

Conclusión(es): Nuestro estudio destaca la metilación alterada de los espermatozoides en iRPL, y sus posibles implicaciones en las vías de desarrollo embrionario y placentario. Los sitios CpG que están hipometilados concretamente en el esperma de la subpoblación iRPL pueden ser evaluados como biomarcadores predictivos.